International Journal of Nanomedicine

Dovepress
open access to scientific and medical research

Open Access Full Text Article

ORIGINAL RESEARCH

Chitosan–tripolyphosphate nanoparticles as *Arrabidaea chica* standardized extract carrier: synthesis, characterization, biocompatibility, and antiulcerogenic activity

This article was published in the following Dove Press journal:
International Journal of Nanomedicine
9 June 2015
Number of times this article has been viewed

Leila Servat-Medina[1,2]
Alvaro González-Gómez[2,3]
Felisa Reyes-Ortega[2]
Ilza Maria Oliveira Sousa[1]
Nubia de Cássia Almeida Queiroz[1]
Patricia Maria Wiziack Zago[1]
Michelle Pedrosa Jorge[1]
Karin Maia Monteiro[1,4]
João Ernesto de Carvalho[1]
Julio San Román[2,3]
Mary Ann Foglio[1]

[1]Chemical, Biological and Agricultural Pluridisciplinary Research Center-State University of Campinas (CPQBA-UNICAMP), Campinas-SP, Brazil; [2]Biomaterials Group, Polymer Science and Technology Institute-Spanish National Research Council (ICTP-CSIC), [3]CIBER-BBN, Centro de Investigación Biomédica en Red, Madrid, Spain; [4]Department of Medical Clinics, Faculty of Medical Sciences, University of Campinas, Campinas-SP, Brazil

Correspondence: Mary Ann Foglio
Chemical, Biological and Agricultural Pluridisciplinary Research Center, State University of Campinas (CPQBA-UNICAMP), Avenida Alexandre Cazelatto 999, 13148-218, Campinas-SP, Brazil
Tel +55 192 139 2861
Fax +55 192 139 2850
Email foglioma@gmail.com

Abstract: Natural products using plants have received considerable attention because of their potential to treat various diseases. *Arrabidaea chica* (Humb. & Bonpl.) B. Verlot is a native tropical American vine with healing properties employed in folk medicine for wound healing, inflammation, and gastrointestinal colic. Applying nanotechnology to plant extracts has revealed an advantageous strategy for herbal drugs considering the numerous features that nanostructured systems offer, including solubility, bioavailability, and pharmacological activity enhancement. The present study reports the preparation and characterization of chitosan–sodium tripolyphosphate nanoparticles (NPs) charged with *A. chica* standardized extract (AcE). Particle size and zeta potential were measured using a Zetasizer Nano ZS. The NP morphological characteristics were observed using scanning electron microscopy. Our studies indicated that the chitosan/sodium tripolyphosphate mass ratio of 5 and volume ratio of 10 were found to be the best condition to achieve the lowest NP sizes, with an average hydrodynamic diameter of 150±13 nm and a zeta potential of +45±2 mV. Particle size decreased with AcE addition (60±10.2 nm), suggesting an interaction between the extract's composition and polymers. The NP biocompatibility was evaluated using human skin fibroblasts. AcE-NP demonstrated capability of maintaining cell viability at the lowest concentrations tested, stimulating cell proliferation at higher concentrations. Antiulcerogenic activity of AcE-NP was also evaluated with an acute gastric ulcer experimental model induced by ethanol and indomethacin. NPs loaded with *A. chica* extract reduced the ulcerative lesion index using lower doses compared with the free extract, suggesting that extract encapsulation in chitosan NPs allowed for a dose reduction for a gastroprotective effect. The AcE encapsulation offers an approach for further application of the *A. chica* extract that could be considered a potential candidate for ulcer-healing pharmaceutical systems.

Keywords: natural product, *Arrabidaea chica*, chitosan, nanoparticle, plant extract, herbal drug, ulcer healing

Introduction

Plants have been a rich source of bioactive compounds for millennia, while the use of plant derivatives for the production of nanobiotechnological products has gained scientific and technological importance in recent years.[1]

Arrabidaea chica (Humb. & Bonpl.) B. Verlot (Bignoniaceae), popularly known as Crajiru, is a native tropical American vine employed in folk medicine for wound healing, inflammation, and gastrointestinal colic.[2] Previous studies with *A. chica* demonstrated in vitro and in vivo healing properties,[3] also increasing collagen content

during the tendon healing process.[4] Antimicrobial,[5] anti-inflammatory,[6] and antioxidant[7] potentials of this species have also been reported.

Applying nanotechnology to plant extracts has revealed an advantageous strategy for herbal drugs considering the numerous features that nanostructured systems have to offer, including solubility, bioavailability, and pharmacological activity enhancement, protection from toxicity, sustained delivery, and protection from physical and chemical degradation.[8,9] Currently, nanotechnological processes involving medicinal plants have provided several innovative delivery systems, including polymeric nanoparticles (NPs). These materials, made from biodegradable and biocompatible polymers such as chitosan (CS), represent an option for controlled drug delivery.[9]

CS, a *N*-deacetylation product of chitin, a natural polysaccharide, is mostly found in the exoskeleton of crustaceans, insects, and fungi.[10] The molecular structure comprises a linear backbone linked through glycosidic bonds with random copolymer of β-(1–4)-linked D-glucosamine and *N*-acetyl-D-glucosamine.[11] Due to the protonation of amino groups, this polysaccharide can form polyelectrolyte complexes with negatively charged compounds. These complexes are formed simultaneously by mixing oppositely charged polyelectrolytes in solution without any chemical covalent cross-linker. In contrast to chemically cross-linked complexes, polyelectrolyte complexes are generally nontoxic, well tolerated, and biocompatible.[10]

Cross-linking CS with sodium tripolyphosphate (TPP) constitutes a mild and efficient method to achieve CS NPs. The particles are formed mainly through the electrostatic interaction between positively charged CS and negatively charged TPP molecules.[12,13]

The biomedical applications of CS include epithelial, bone, and dental tissue regeneration, wound dressing, drug delivery, as well as antimicrobial, antioxidant, and anti-inflammatory properties.[14–17] There is strong evidence of CS nanocarrier potential for many challenging drug delivery applications. Moreover, there is also indicative data regarding CS biocompatibility, which further supports the potential use in nanomedicine.[11] The present research was conducted to formulate and develop strategies to improve the therapeutic efficacy of *A. chica* standardized extract employing CS NPs as a carrier. The process parameters were adjusted to achieve the best conditions for NP production. The NP system's biocompatibility was evaluated using human fibroblasts. Gastric ulcer experimental models in rats were used to evaluate the antiulcerogenic activity of *A. chica* NPs.

Materials and methods

Plant material

A. chica Verlot (Bignoniaceae) leaves were collected at Chemical, Biological and Agricultural Pluridisciplinary Research Center, State University of Campinas experimental field (22°45′00″ south and 47°10′21″ west; Paulinia, Brazil). The corresponding voucher specimen (1348) was deposited at CPQBA-Herbarium. Genetic patrimony number authorization 010150/2012-9 was issued by Conselho Nacional para o Desenvolvimento Científico e Tecnológico (CNPq) for this study.

Extraction procedures

A. chica hydroalcoholic standardized extract (AcE) was obtained according to the method described by Jorge et al[3] and Paula et al[18] with modifications. One kilogram of dried and ground leaves were extracted three times, using 5 L of acidified (0.3% citric acid) 70% hydroethanol solution throughout 1.5-hour periods, at room temperature, with mechanical stirring. The procedure was repeated a further couple of times. The extract was filtered and the organic solvent was removed under vacuum. The resulting crude extract was further dried using a Mini Spray Drier B-290, loop B-295 (BÜCHI Labortechnik AG, Flawil, Switzerland). The inlet temperature was 100°C±2°C and the outlet temperature was 60°C±2°C, with 250 mL·hour^{-1} aspiration flow with N_2, 414 L·hour^{-1} injection pressure, and 5 mL·minute^{-1} feed flow at room temperature.

Phytochemical analysis

Analytical analysis was adapted from a previously described method by Wen et al[19] performed with a Shimadzu series high-pressure liquid chromatography (HPLC) system equipped with an online degasser (DUG-2A), quaternary pump (LC-10AT), autosampler (SIL 20A HT), column heater (CTO 10AS Vp), and photodiode array detector (DAD) (SPD-M10Vp) (Shimadzu Corporation, Kyoto, Japan). Instrument control and data analysis were carried out using Class VP 6.13 edition; C18 columns were used (5 µm, 4.6×250 mm; Gemini®; Phenomenex, Torrance, CA, USA). The flow rate of the mobile phase was kept at 1.0 mL·minute^{-1}. Mobile phase A was water that contained 0.2% H_3PO_4, and phase B was methanol. The gradient conditions were as follows: 0–5 mintues, 45% phase B; 5–10 minutes, 90% phase B; 10–16 minutes, 30%–45% phase B; 16–18 minutes, 45% phase B; 18–25 minutes, 45%–80% phase B; 20–30 minutes, 100% phase B; and 30–45 minutes, 45% phase B. The column temperature was controlled at

35°C. The injection volume was 20 µL. The detection DAD wavelength was set at 470 nm.

Preparation of CS-TPP NPs

CS-TPP NPs were prepared according to the ionic gelation method.[12] Briefly, 1% (w/v) CS solutions were prepared by dissolving CS (PROTASAN UP CL 213; molecular weight >150 kDa, 87% deacetylated; FMC BioPolymer AS, Sandvika, Norway) into Milli-Q® water. To evaluate the influence of the cross-linking agent concentration, different amounts of TPP (Sigma-Aldrich Co., St Louis, MO, USA) were dissolved in Milli-Q® water to form TPP solutions. NPs were formed by adding TPP solution dropwise onto a CS solution under mechanical stirring (ULTRA-TURRAX®) (7,200 rpm). Thereafter, the CS-TPP particle suspension was processed under ultrasonication (Sonics VC 750) for 5 minutes, producing CS particles with controlled particle sizes.

AcE encapsulation

AcE was incorporated into the TPP solution prior to NP formation. AcE was added in different concentrations of 10%, 15%, or 25% with respect to the total amount of CS used for particle preparation. The NP dispersion was dialyzed against distilled water for 24 hours using a cellulose membrane (Spectra/Por dialysis membrane; molecular weight cutoff of 3,500 Da) to remove the nonencapsulated AcE. The amount of nonentrapped AcE recovered in the external aqueous phase after dialysis was quantified using a calibration curve obtained from different AcE solutions of known concentration, by measuring absorbance of the external aqueous dialyzed solution at 485 nm on a PerkinElmer Instrument spectrometer Lambda 35 ultraviolet–visible spectrophotometer (PerkinElmer Inc., Waltham, MA, USA). The percentage of encapsulate efficiency (EE) was defined as:

$$\%EE = \{[(AcE)_o - (AcE)_i]/(AcE)_o\} \times 100 \quad (1)$$

where $(AcE)_o$ is the total AcE amount added and $(AcE)_i$ is the nonencapsulated AcE amount. The sponges were prepared by the direct freeze–drying[20] of NP dispersions.

Measurement of NP size and zeta potential

Measurement of the average particle size and particle size distribution, polydispersity index, and zeta potential (ZP) of CS-TPP NPs was performed using a Zetasizer Nano ZS (Malvern Instruments, Malvern, UK). Hydrodynamic diameter and polydispersity index were determined by dynamic light scattering. The intensity of light scattered was used to calculate the mean hydrodynamic diameter (*Z*-average mean), based on the Stokes–Einstein equation, which assumes that the particle is spherical. For each sample, the data average and standard deviation (SD) were calculated from at least five measurements.

ZP analysis was carried out using laser doppler electrophoresis with 20 runs per measurement at 25°C. The ZPs were automatically calculated from the electrophoretic mobility using the Smoluchowski's approximation:

$$UE = 2*\varepsilon*z*f(ka)/3*\eta \rightarrow z \approx UE*\eta/\varepsilon \quad (2)$$

where UE is the electrophoretical mobility, ε is the dielectric constant, z is the ZP, f(ka) is Henry's function, and η is the viscosity. This approximation is generally applied when the measurements are carried out in aqueous media, and it considers that Henry's function takes a value of 3/2.

Morphology observation

The morphological characteristics of NPs were observed using a Hitachi SU8000 UHR Cold-Emission FE-SEM apparatus (Hitachi Ltd., Tokyo, Japan). Scanning electron microscopy (SEM) images were obtained using an accelerating voltage of 3 keV. Samples were prepared by deposition of the corresponding NP suspension (100 µL) over small glass disks (13 mm in diameter and 1 mm thick), and the solvent (H_2O) was evaporated at room temperature. Finally, the samples were coated with chrome prior to examination.

Cell culture conditions

The biological response was tested with human embryonic skin fibroblasts (Innoprot, Biscay, Spain). The culture medium was Dulbecco's Modified Eagle's Medium (DMEM) enriched with 4,500 mg·mL^{-1} glucose (Sigma-Aldrich Co.) supplemented with 10% fetal bovine serum (FBS), 200 mM L-glutamine, 100 units·mL^{-1} penicillin, and 100 mg·mL^{-1} streptomycin, modified with HEPES (complete medium). The culture medium was carefully changed at selected times to avoid any disturbance to the culture conditions. Cells without treatment were used as a negative control.

Cell viability assay

Cell viability (CV) of NP, AcE-NP, and AcE was assessed by a 3-(4,5-dimethylthiazol-2-yl)-2,5 diphenyltetrazolium bromide (MTT) assay.[21,22] The AcE concentration tested corresponded to the amount of AcE loaded in the NPs (ratio of 20%). To evaluate the possibility of cytotoxic product

formation, the samples were set up in 5 mL of FBS-free supplemented DMEM and placed on a shaker at 37°C. The conditioned medium was collected and filtered at days 1, 2, 3, 7, 10, 15, 21 and stored at −20°C until required. Fibroblasts were seeded at a density of 8×10^4 cells·mL^{-1} in complete medium into a sterile 96-well plate and incubated to confluence. CV was determined for the different NP concentrations (0.001–0.5 g·mL^{-1}) in 1% FBS supplemented with DMEM. After 24 hours, the medium was replaced with the corresponding sample and incubated at 37°C in humidified air with 5% CO_2 for 24 hours, 48 hours, or 72 hours. An MTT solution (0.5 mg·mL^{-1}) was prepared in warm FBS-free supplemented DMEM and plates were incubated at 37°C for 3–4 hours. Excess medium and MTT were removed and dimethyl sulfoxide (100 µL) was added to all wells in order to dissolve MTT taken up by the cells. Finally, the absorbance was measured with a BioTek Synergy HT detector using a test wavelength of 570 nm. CV (%) was calculated with the following equation:

$$CV\ (\%) = 100 \times [(OD_S - OD_B)/(OD_C - OD_B)]. \quad (3)$$

OD_S, OD_B, and OD_C are defined as the optical density for sample (S), blank (B) (culture medium without cells), and control (C), respectively.

Animals

Adult male Wistar/Uni rats (200–300 g) were obtained from the Multidisciplinary Center for Biological Investigation on Laboratory Animals Sciences (CEMIB-UNICAMP). The animals were maintained at the animal facilities of the Pharmacology and Toxicology Division, CPQBA, University of Campinas (Campinas, Brazil) under controlled conditions (22°C±3°C, in a 12-hour light/dark cycle, with free access to food and water). Animal care, research, and animal euthanasia protocols were performed in accordance with the principles and guidelines adopted by the Brazilian College of Animal Experimentation (COBEA) and approved by the Institute of Biology/UNICAMP – Ethical Committee for Animal Research (number 1900-1). Prior to the experimental tests, rats were fasted for 12 hours with water ad libitum. Ultrasonication of freeze-dried particles (sponge) in saline provided the NP samples used in both tests.

Ethanol-induced gastric ulcer

Animals were separated into six groups (number [n]=6) and orally treated with saline (NaCl 0.9%) 10 mL·kg^{-1}, carbenoxolone 200 mg·kg^{-1}, nonloaded NPs 300 mg·kg^{-1}, and *A. chica* NPs in three different doses (30 mg·kg^{-1}, 100 mg·kg^{-1}, or 300 mg·kg^{-1}). One hour after treatment, all rats orally received 1 mL of absolute ethanol. After 1 hour, the animals were euthanized by an overdose of thiopental and their stomachs were removed, by opening them along the greater curvature, and washed. After washing the stomachs with saline solution, the ulcerative lesion index (ULI) was scored as described by Vendramini-Costa et al[23] using the arbitrary scoring system shown in Table 1. Gastroprotection was calculated by comparing the treatment group with the negative control (saline solution) group, using the following formula:

$$\text{Gastroprotection (\%)} = \frac{\text{Average control} - \text{average treatment}}{\text{Average control}} \times 100. \quad (4)$$

Indomethacin-induced gastric ulcer

Rats were distributed into three groups (n=6) according to the treatment employed: saline (NaCl 0.9%) 10 mL·kg^{-1}, ranitidine 50 mg·kg^{-1}, and *A. chica* NPs 200 mg·kg^{-1}. One hour after oral treatment, animals received an intraperitoneal dose of indomethacin (30 mg·kg^{-1}). After 6 hours, the rats were euthanized by an overdose of thiopental. The stomachs were removed, by opening them along the greater curvature, and washed. After washing the stomachs with saline solution, the ULI was calculated as described in the ethanol-induced gastric ulcer procedure.

Statistical analysis

The CV results are presented as the mean ± SD (n=8). Averages were compared by one-way analysis of variance (ANOVA) followed by *t*-tests. Data from the ulcer experimental test are shown as the mean ± standard error of the mean of the six animals per group. Averages were compared by ANOVA followed by Tukey's post hoc test for multiple comparisons. Differences were considered significant if the *P*-value was <0.05.

Table 1 Scoring system employed for the determination of the ulcerative lesion index in gastric ulcer induction models

Parameter	Score
Loss of normal morphology	1
Discoloration of mucosa	1
Edema	1
Hemorrhages	1
Petechial points (≤10)	2
Petechial points (>10)	3
Ulcers up to 1 mm	n×2
Ulcers >1 mm	n×3
Perforated ulcers	n×4

Abbreviation: n, number of ulcers found.

Results and discussion

Phytochemical analysis

Standardization of plant inputs for the pharmaceuticals industry plays an important role in product outcomes. Factors such as soil, climate conditions, genotypes, harvesting, and postharvest conditions have been shown to have an important influence on both chemical and biological activity. Therefore, the quality of the botanical material, as well as the adequate processing of the fresh material, including drying, transportation, storage, and the use of appropriate and reproducible extraction techniques have a straight outcome on health benefits and economic issues.[24] Previous studies were conducted to determine the best conditions for AcE preparation.[3,18,25–27] Anthocyanins are the most common pigments in nature and can be extracted with acidified solvents such as water, acetone, ethanol, methanol, or mixtures of aqueous solvents.[28] The crude extract was obtained using a 70% ethanol solution with 0.3% citric acid. Methanol is indeed the most common and effective solvent for extracting anthocyanins; however, it is an environmental pollutant and it is also more toxic than other alcohols. Thus, ethanol is preferred over methanol for the extraction of anthocyanins from plant material.[28] Citric acid is important for stabilizing anthocyanin in the normal extraction process without interfering with the pharmacological activity. Barros et al[29] reported that citric acid was capable of improving 3-deoxyanthocyanidin extraction yield.

The presence of 6,7,3′,4′-tetrahydroxy-5-methoxyflavylium, 6,7,4′-trihydroxy-5-methoxyflavylium, and carajurin (Figure 1), compounds with straight relationship with *A. chica* extract activity,[26] was monitored by HPLC-DAD analysis. The carajurin content was determined as 6.51%±0.07% yield.

Preparation of CS-TPP NPs

Ionotropic gelation involves the spontaneous aggregation of CS with multivalent counter ions, most commonly TPP. NPs were formed immediately upon mixing TPP and CS solutions as molecular linkages between TPPs and CS amino groups.[30,31] The adjustment of parameters such as CS concentration, the CS:TPP polymer ratio, and mixing conditions control CS-TPP NP size.[32–34]

Initial studies aiming to optimize NP formation were conducted. Particle size and particle size and polydispersity were measured with a Zetasizer Nano. Particles of 150 nm were produced by employing a CS-TPP mass ratio of 5. Mass ratios of 7, 10, or 20 resulted in particles 387–681 nm in size (Table 2).

Particle size increased with an increasing CS-TPP mass ratio, as described by Gan et al[30] and Li and Huang;[35] this is oppossed to data reported by Konecsni et al.[36] The NP suspension became turbid as the CS-TPP mass ratio was reduced to 1, indicating the production of large particles. A similar phenomenon was observed by Hu et al[37] where aggregates with a large diameter were formed when the CS-TPP mass ratio was decreased to 1.5. The optimized CS-TPP mass ratio was reported as 5[37] and 3.75.[35] Our studies indicated that CS concentrations of 1 mg·mL^{-1}, with a CS-TPP polymer ratio (w:w) of 5, a CS-TPP volume ratio of 10, and using mechanical stirring at 7,200 rpm, followed by sonication (5 minutes, 20% amplitude) resulted in the reproducible formation of NPs with an average hydrodynamic diameter of 150±13 nm and a ZP of +45±2 mV, with high yields (75%).

The ZP reflects the electrical superficial charge of particles and is influenced by the particle composition and the dispersion medium.[38] This parameter is used as a NP stability index. The electronic repulsion between particles can greatly affect the particle stability in suspension. As a result, a higher absolute ZP value indicates a more stable suspension, whereas a lower value implicates colloid instability, which could lead to NP aggregation.[39] NPs with a ZP above ±30 mV have shown to be stable in suspension, as the surface charge prevents aggregation of the particles.[38]

Encapsulation of *A. chica* extract

AcE was added to TPP aqueous solution in different concentrations in relationship to CS (w/w) for AcE-NP production. The size, polydispersity index, and ZP were measured by a Zetasizer Nano (Malvern Instruments) (Table 3).

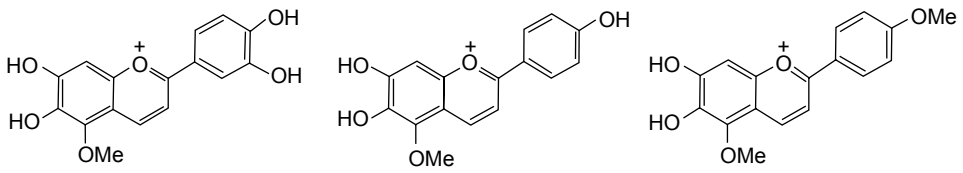

Figure 1 Chemical structure of 3-deoxyanthocyanidins: pigment 1 (6,7,3′,4′-tetrahydroxy-5-methoxyflavylium), pigment 2 (6,7,4′-trihydroxy-5-methoxyflavylium), and pigment 3 (carajurin).

Table 2 Average particle size and polydispersity measured with a Zetasizer Nano (Malvern Instruments, Malvern, UK)

CS-TPP mass ratio	Size (nm)	Polydispersity
20	681±16	0.59±0.1
10	473±8	0.24±0.03
7	387±10	0.26±0.04
5	150±13	0.18±0.02
4	230±15	0.23±0.05

Notes: Values are shown as the mean ± standard deviation; n=5.
Abbreviations: CS, chitosan; TPP, sodium tripolyphosphate; n, number.

The particle size decreased with AcE concentration increases, suggesting an interaction between the extract's composition and the polymers. A similar effect was reported for *Camellia sinensis* catechins. According to Hu et al,[37] the mean diameter of CS-TPP NPs loaded with *C. sinensis* catechins was smaller to that of the corresponding CS-TPP NPs, which may be attributable to a greater cross-linking density of the tea catechin-loaded NPs caused by the interactions between the CS matrix and catechins.

The ZP values were positive for all compositions, indicating a positively charged surface. The NPs demonstrated higher +30 mV ZP, ensuring particle stability.

Encapsulation efficiency

The measurement of the amount of the drug released (nonentrapped AcE) in the external aqueous solution recovered after NP dialysis permitted the determination of AcE entrapped within the polymeric NPs as 84% yield. Considering the AcE amount added during NP production and the EE, the ratio of AcE loaded in the NPs was 20%.

Evidence for the encapsulation of AcE was provided by Fourier transform infrared spectroscopy (Supplementary materials, Figure S1).

Morphological characteristics of AcE-NP and sponges

The NPs were predominantly spherical (Figure 2). The size was approximately 60 nm, which is consistent with the results obtained by light scattering.

Table 3 Average particle size, polydispersity index, and zeta potential values measured with a Zetasizer Nano (Malvern Instruments, Malvern, UK)

Proportion of CS/AcE	Size (nm)	Polydispersity	Zeta potential (mV)
Without AcE	150±13	0.18±0.02	+45.0±2
10%	153±9.3	0.24±0.03	+32.7±1.8
15%	125±7.8	0.26±0.04	+32.1±0.8
25%	60±10.2	0.3±0.1	+32.9±1.5

Notes: Values are shown as the mean ± standard deviation; n=5.
Abbreviations: CS, chitosan; AcE, *Arrabidaea chica* extract; n, number.

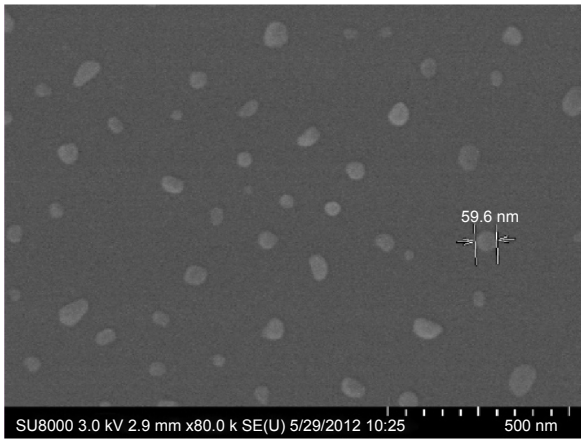

Figure 2 Images of *Arrabidaea chica* nanoparticles obtained by scanning electron microscopy.

The NP dispersion was directionally frozen in liquid nitrogen and then freeze-dried, forming sponge-like structures. The sponge's morphology was determined by SEM, by direct surface analysis (Figure 3). Some groups[40–42] have reported the preparation of porous structures via unidirectional freezing, where the physics of ice formation can be used to develop sophisticated porous materials with a process that does not involve any chemical reaction. The method consists of freezing the colloidal aqueous suspensions. This relatively simple technique has the potential to produce complex, multicomponent, aligned structures for several applications.

CS sponges have been widely used as tissue engineering scaffolds, owing to their simple fabrication, efficient aqueous absorption, and porous structure enabling cell penetration.[43] Noel et al[44] and Smith et al[45] suggested the possibility of using a CS sponge device as an alternative to deliver antibiotics locally as an adjunctive therapy for the treatment and prevention of infections, from open traumatic

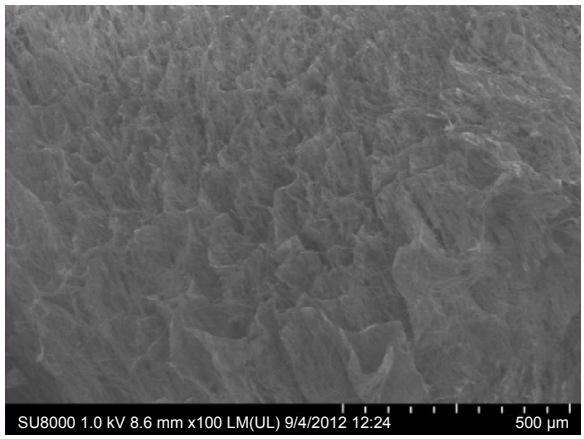

Figure 3 Scanning electron micrograph of freeze-dried *Arrabidaea chica* nanoparticles (sponge).

wounds to prophylactic use in surgical sites. Furthermore, a CS sponge can be used as a drug reservoir[43] or a storage form for CS systems. The sponges reported herein were used as an NP storage form; therefore, they can return to the NPs through ultrasonication. Additional studies will be required to determine the best conditions to prepare CS standardized scaffolds.

Biocompatibility of NPs

One of the most popular and convenient ways to determine CV is the rapid colorimetric tetrazolium dye procedure commonly referred to as the MTT assay. This assay is based on the cleavage of the yellow-colored tetrazolium salt, 3-(4,5-dimethylthiazol-2-yl)-2,5-diphenyl tetrazolium bromide, into a blue-colored formazan by the mitochondrial enzyme succinate-dehydrogenase.[46]

In order to disregard any cytotoxic product's influence on fibroblast proliferation, an MTT assay was conducted with NPs, AcE-NPs, and AcE (0.5 mg·mL^{-1}) that stayed in contact with the culture medium for determined time periods (1–21 days). The results are shown in Figure 4.

The CV was approximately or higher than 80% in all cases; according to assessment of the standard ISO 10993-5:2009,[47] biocompatibility was not compromised. Thus, under the experimental conditions, the samples did not produce cytotoxic products.

To evaluate the sample's CV by direct contact, an MTT assay was conducted in which the fibroblasts were exposed to samples by 24 hours, 48 hours, or 72 hours (Figure 5). The NPs, AcE-NPs, and AcE at 0.001–0.125 mg·mL^{-1} concentrations showed the same viability profile of approximately 100%.

The 30% CV, which is in comparison to the control of AcE at 0.5 mg·mL^{-1}, might have a relationship with the antioxidant components of the extract. According to Heim et al,[48] pro-oxidant effects have shown to be involved with cytotoxic and proapoptotic effects of flavonoids isolated from plants. Therefore, this information suggests that a molecule with the same chemical structure can optimize antioxidant capacity and it may also exacerbate oxidative stress and damage to functional and structural cellular molecules.[48] However, considering the role of flavonoid's radical stability in pro-oxidant behavior postulated by Bors et al[49] structural advantages to radical stability that increase antioxidant activity, such as a 3′4′-catechol, 3-OH, and conjugation between the A- and B-rings, may modulate the adverse oxidative effects of flavonoids.

Pro-oxidant properties seem to have a direct relationship with flavonoid concentration.[50] At a concentration of 0.250 mg·mL^{-1}, *A. chica* free extract demonstrated 90% CV, whereas at 0.5 mg·mL^{-1}, CV decrease to 20%. A study described by Procházková et al[50] reported that 1–50 µM of quercetin decreased DNA oxidative damage, whereas 100 µM increased damage. This observation demonstrated the pro-oxidative effect of the highest concentration employed. Nevertheless, quercetin maintained the antioxidant activity when encapsulated in the CS-TPP NPs.[51]

Herein, AcE-NPs showed different behavior when compared to the free extract, demonstrating the capability of maintaining CV at the lowest concentrations tested; likewise, they stimulated cell proliferation at higher concentrations, confirming the positive association of nanotechnology with herbal medicine. The AcE-NP proliferative activity indicated

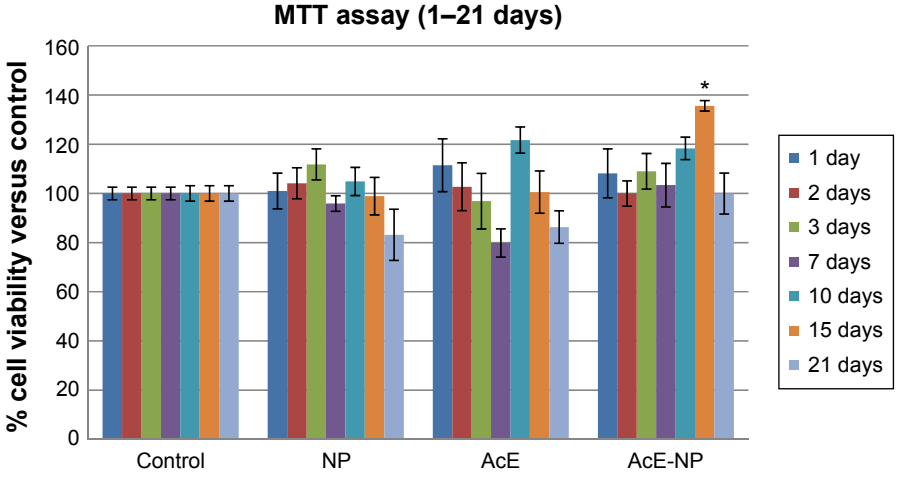

Figure 4 Fibroblast viability in the presence of chitosan NPs, AcE, or AcE-NP at 0.5 mg·mL^{-1}.
Notes: Data are presented as the mean ± standard deviation (n=8). Statistical analysis was performed using a one-way ANOVA followed by a Student's *t*-test. *Significant difference between the AcE-NP and the control was $P<0.05$.
Abbreviations: NP, nanoparticle; AcE, *Arrabidaea chica* extract; AcE-NP, *Arrabidaea chica* extract nanoparticle; n, number; ANOVA, analysis of variance.

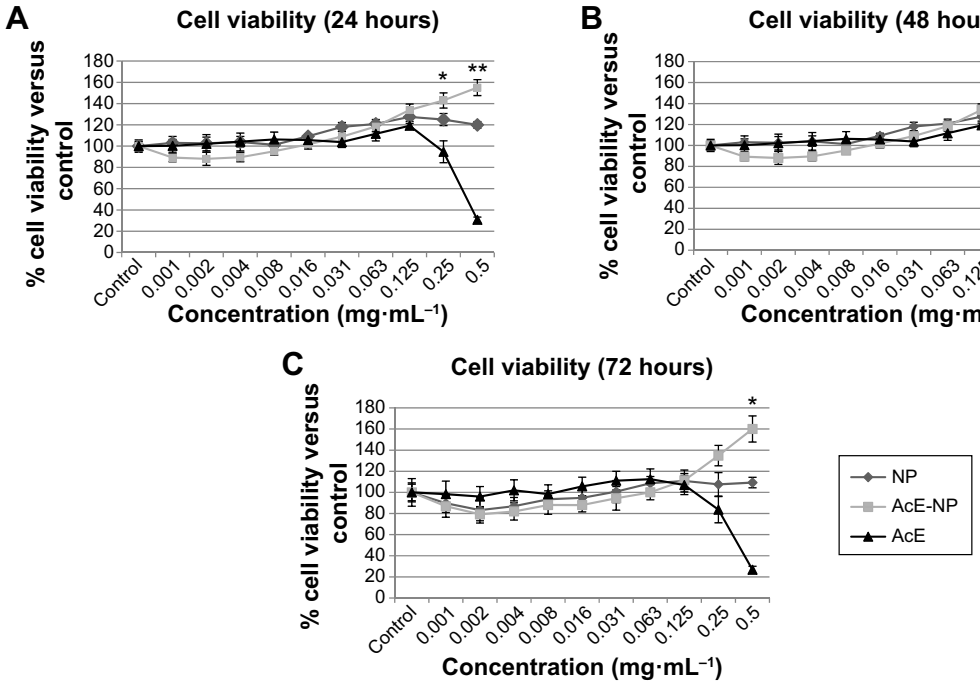

Figure 5 Fibroblast viability in relation to 24-hour, 48-hour, or 72-hour exposure to chitosan NPs, AcE, or AcE-NPs.
Notes: (**A**) 24 hours; (**B**) 48 hours; (**C**) 72 hours. Data are shown as the mean ± standard deviation (n=8). Statistical analysis was performed using a one-way ANOVA followed by a Student's *t*-test. *$P<0.01$; **$P<0.001$.
Abbreviations: NP, nanoparticle; AcE-NP, *Arrabidaea chica* extract nanoparticle; AcE, *Arrabidaea chica* extract; n, number; ANOVA, analysis of variance.

that AcE encapsulation in CS NPs may be a useful approach for improving *A. chica* biocompatibility.

Antiulcerogenic activity

The antiulcerogenic activity of *A. chica* NPs was evaluated with acute gastric ulcers induced by ethanol and indomethacin experimental models.

The acute lesions on the gastric mucosa caused by ethanol ingestion involve mucus destruction and the release of free radicals, playing a vital role in altering the stomach's natural defense mechanisms. The ethanol-induced gastric ulcer experimental model is a simple and reproducible procedure and, therefore, may be considered a test of choice for screening samples with possible antiulcerogenic effects.[52,53]

The gastroprotective activity of *A. chica* extract in ethanol-induced ulcer formation in rats was previously reported by Jorge,[54] employing 100 mg·kg^{-1}, 300 mg·kg^{-1}, and 1,000 mg·kg^{-1} doses, revealing 125 mg·kg^{-1} as the effective dose to promote 50% gastroprotection. Herein, CS NPs loaded with *A. chica* extract reduced the ULI using lower doses (30 mg·kg^{-1}, 100 mg·kg^{-1}, and 300 mg·kg^{-1}). The 30 mg·kg^{-1} dose was sufficient to reduce 58% of the ULI in comparison to the control group (saline) (Figure 6, Figure S2).

The doses used in the present research refer to the amount of NPs. Therefore, when extrapolating the amount of *A. chica* loaded in those particles, the amount of tested plant extract is considerably smaller. The proportion of *A. chica* extract present in the NPs was 20%; that is, the highest tested dose (300 mg·kg^{-1}) corresponded to approximately 60 mg·kg^{-1} of plant extract. These results suggest that extract encapsulation in CS NPs allows for a dose reduction for the same

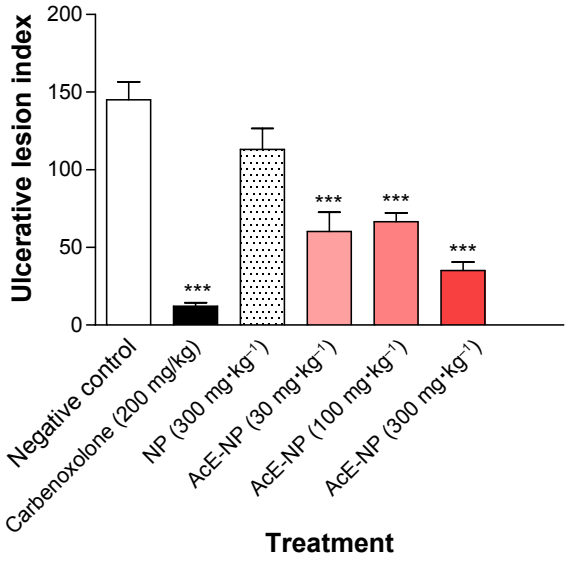

Figure 6 Ulcerative lesion index of nonloaded NPs and AcE-NP on ethanol-induced gastric ulceration in rats.
Notes: Data are shown as the mean ± standard error (n=6). Statistical analysis was performed using a one-way ANOVA followed by Tukey's test. ***$P<0.001$ compared with negative control (saline). Carbenoxolone was used as a positive control.
Abbreviations: NP, nanoparticle; AcE-NP, *Arrabidaea chica* extract nanoparticle; n, number; ANOVA, analysis of variance.

pharmacological gastroprotective effect when compared to the free extract.

A similar phenomenon was described by Strasser et al[55] where the nanoencapsulated *Passiflora serratodigitata* L. extract had greater antiulcerogenic activity than their conventional extract forms.

In order to evaluate the gastroprotective effect of the *A. chica* NPs through a systemic gastric ulcer model, an indomethacin-induced gastric ulcer was performed. The integrity of gastric mucosa against ulcerogenic and necrotizing agents depends on the generation of prostaglandins by cyclooxygenase-1 (COX-1). Indomethacin is a nonsteroidal anti-inflammatory drug that potently damages prostaglandin synthesis by COX inhibition.[56] The gastroprotective effect of the *A. chica* NPs (200 mg·kg^{-1}) reduced 58% of the nonsteroidal anti-inflammatory drug-induced lesion when compared to the negative control group (Figure 7).

The pharmacological effect of *A. chica* NPs in both ethanol- and indomethacin-induced gastric ulcer models represents promising results and, therefore, deserves further investigation.

Nanostructured systems might be able to potentiate the action of plant extracts, reducing the required dose and side effects, thus improving activity.[9] The AcE-NP antiulcer effect indicated that AcE encapsulation in CS NPs may be an useful approach for improving *A. chica* applicability for ulcer-healing pharmaceutical systems.

Conclusion

The CS-TPP NPs and CS-TPP NPs loaded with AcE were successfully prepared based on the ionic gelation between CS and TPP. The CS-TPP mass ratio of 5 and volume ratio of 10 were found to be the best condition to achieve the lowest NP sizes. Particle size decreased with AcE addition, suggesting an interaction between the extract's composition and polymers. The *A. chica* NPs showed good biocompatibility, which was demonstrated in CV studies and antiulcerogenic activity in rat experimental models. The AcE encapsulation offers an approach for the further application of *A. chica* extract that could be considered a potential candidate for ulcer-healing pharmaceutical systems.

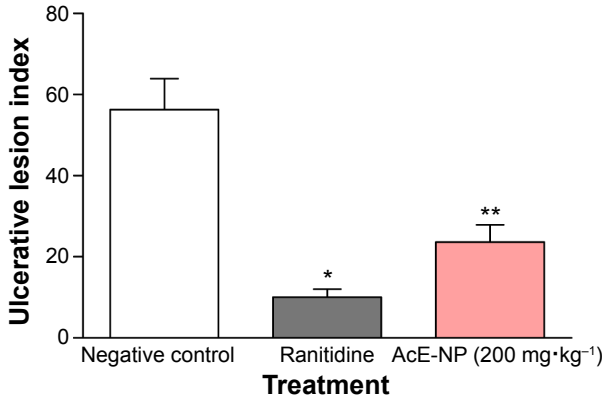

Figure 7 Ulcerative lesion index of AcE-NP on indomethacin-induced gastric ulceration in rats.

Notes: Data are shown as the mean ± standard error (n=6). Statistical analysis was performed using a one-way ANOVA followed by Tukey's test. *$P<0.001$; **$P<0.01$ compared with negative control (saline). Ranitidine was used as a positive control.

Abbreviations: AcE-NP, *Arrabidaea chica* extract nanoparticle; n, number; ANOVA, analysis of variance.

Acknowledgments

We gratefully acknowledge the financial support received from the Fundação de Amparo à Pesquisa do Estado de São Paulo (Fapesp grant #2009/16484-1; 2010/07781-0; 2009/51020-6; 2011/09127-8) and Conselho Nacional para o Desenvolvimento Científico e Tecnológico (CNPq).

Disclosure

The authors report no conflicts of interest in this work.

References

1. Joanitti GA, Silva LP. The emerging potential of by-products as platforms for drug delivery systems. *Curr Drug Targets*. 2014;15(5):478–485.
2. Zorn B, García-Piñeres AJ, Castro V, Murillo R, Mora G, Merfort I. 3-Desoxyanthocyanidins from *Arrabidaea chica*. *Phytochemistry*. 2001; 56(8):831–835.
3. Jorge MP, Madjarof C, Gois Ruiz AL, et al. Evaluation of wound healing properties of *Arrabidaea chica* Verlot extract. *J Ethnopharmacol*. 2008;118(3):361–366.
4. Aro AA, Simões GF, Esquisatto MA, et al. *Arrabidaea chica* extract improves gait recovery and changes collagen content during healing of the Achilles tendon. *Injury*. 2013;44(7):884–892.
5. Höfling JF, Anibal PC, Obando-Pereda GA, et al. Antimicrobial potential of some plant extracts against Candida species. *Braz J Biol*. 2010;70(4):1065–1068.
6. de Oliveira DPC, Borrás MRL, de Lima Ferreira LC, López-Lozano JL. [Anti-inflammatory activity of the aqueous extract of *Arrabidaea chica* (Humb. & Bonpl.) B. Verl. on the self-induced inflammatory process from venoms amazonians snakes]. *Revista Brasileira de Farmacognosia*. 2009;19(2b):643–649. Portuguese.
7. Siraichi JT, Felipe DF, Brambilla LZ, et al. Antioxidant capacity of the leaf extract obtained from *Arrabidaea chica* cultivated in Southern Brazil. *PLoS One*. 2013;8(8):e72733.
8. Ajazuddin, Saraf S. Applications of novel drug delivery system for herbal formulations. *Fitoterapia*. 2010;81(7):680–689.
9. Bonifácio BV, Silva PB, Ramos MA, Negri KM, Bauab TM, Chorilli M. Nanotechnology-based drug delivery systems and herbal medicines: a review. *Int J Nanomedicine*. 2014;9:1–15.
10. Luo Y, Wang Q. Recent development of chitosan-based polyelectrolyte complexes with natural polysaccharides for drug delivery. *Int J Biol Macromol*. 2014;64:353–367.
11. Garcia-Fuentes M, Alonso MJ. Chitosan-based drug nanocarriers: where do we stand? *J Control Release*. 2012;161(2):496–504.
12. Calvo P, Remuñán-López C, Vila-Jato JL, Alonso MJ. Novel hydrophilic chitosan-polyethylene oxide nanoparticles as protein carriers. *J Appl Polym Sci*. 1997;63(1):125–132.
13. Zamora-Mora V, Fernández-Gutiérrez M, San Román J, Goya G, Hernández R, Mijangos C. Magnetic core-shell chitosan nanoparticles: rheological characterization and hyperthermia application. *Carbohydr Polym*. 2014;102:691–698.

14. Girones Molera J, Mendez JA, San Roman J. Bioresorbable and non-resorbable polymers for bone tissue engineering. *Curr Pharm Des*. 2012;18(18):2536–2557.
15. Muzzarelli RA, El Mehtedi M, Mattioli-Belmonte M. Emerging biomedical applications of nano-chitins and nano-chitosans obtained via advanced eco-friendly technologies from marine resources. *Mar Drugs*. 2014;12(11):5468–5502.
16. Mogoşanu GD, Grumezescu AM. Natural and synthetic polymers for wounds and burns dressing. *Int J Pharm*. 2014;463(2):127–136.
17. Gomathysankar S, Halim AS, Yaacob NS. Proliferation of keratinocytes induced by adipose-derived stem cells on a chitosan scaffold and its role in wound healing, a review. *Arch Plast Surg*. 2014;41(5):452–457.
18. Paula JT, Paviani LC, Foglio MA, Sousa IMO, Cabral FA. Extraction of anthocyanins from *Arrabidaea chica* in fixed bed using CO_2 and CO_2/ethanol/water mixtures as solvents. *J Supercrit Fluids*. 2013;81:33–41.
19. Wen D, Li C, Di H, Liao Y, Liu H. A universal HPLC method for the determination of phenolic acids in compound herbal medicines. *J Agric Food Chem*. 2005;53(17):6624–6629.
20. Peniche C, Fernández M, Rodríguez G, et al. Cell supports of chitosan/hyaluronic acid and chondroitin sulphate systems. Morphology and biological behaviour. *J Mater Sci Mater Med*. 2007;18(9):1719–1726.
21. Mosmann T. Rapid colorimetric assay for cellular growth and survival: application to proliferation and cytotoxic assays. *J Immunol Methods*. 1983;65(1–2):55–63.
22. Denizot F, Lang R. Rapid colorimetric assay for cell growth and survival. Modifications to the tetrazolium dye procedure giving improved sensitivity and reliability. *J Immunol Methods*. 1986;89(2):271–277.
23. Vendramini-Costa DB, Monteiro KM, Iwamoto LH, et al. Gastroprotective effects of goniothalamin against ethanol and indomethacin-induced gastric lesions in rats: Role of prostaglandins, nitric oxide and sulfhydryl compounds. *Chem Biol Interact*. 2014;224C:206–212.
24. Heinrich M, Barnes J, Gibbons S, Williamson EM. *Fundamentals of Pharmacognosy and Phytotherapy*. London, UK: Elsevier; 2007.
25. Figueira GM, Ramelo PR, Ogasawara DC, et al. A set of microsatellite markers for *Arrabidaea chica* (Bignoniaceae), a medicinal liana from the Neotropics. *Am J Bot*. 2010;97(7):e63–e64.
26. Taffarello D, Jorge MP, Sousa IMO, et al. [Activity of *Arrabidaea chica* (Humb. & Bonpl.) Verlot extracts obtained by biotechnological processes on fibroblast and human tumor cells]. *Química Nova*. 2013;36(3):431–436. Portuguese.
27. Aro AA, Freitas KM, Foglio MA, et al. Effect of the *Arrabidaea chica* extract on collagen fiber organization during healing of partially transected tendon. *Life Sci*. 2013;92(13):799–807.
28. Khoddami A, Wilkes MA, Roberts TH. Techniques for analysis of plant phenolic compounds. *Molecules*. 2013;18(2):2328–2375.
29. Barros F, Dykes L, Awika JM, Rooney LW. Accelerated solvent extraction of phenolic compounds from sorghum brans. *J Cereal Sci*. 2013;58(2):305–312.
30. Gan Q, Wang T, Cochrane C, McCarron P. Modulation of surface charge, particle size and morphological properties of chitosan-TPP nanoparticles intended for gene delivery. *Colloids Surf B Biointerfaces*. 2005;44(2–3):65–73.
31. Lai P, Daear W, Löbenberg R, Prenner EJ. Overview of the preparation of organic polymeric nanoparticles for drug delivery based on gelatine, chitosan, poly(d,l-lactide-co-glycolic acid) and polyalkylcyanoacrylate. *Colloids Surf B Biointerfaces*. 2014;118:154–163.
32. Nasti A, Zaki NM, de Leonardis P, et al. Chitosan/TPP and chitosan/TPP-hyaluronic acid nanoparticles: systematic optimisation of the preparative process and preliminary biological evaluation. *Pharm Res*. 2009;26(8):1918–1930.
33. Dong Y, Ng WK, Shen S, Kim S, Tan RB. Scalable ionic gelation synthesis of chitosan nanoparticles for drug delivery in static mixers. *Carbohydr Polym*. 2013;94(2):940–945.
34. Fàbregas A, Miñarro M, García-Montoya E, et al. Impact of physical parameters on particle size and reaction yield when using the ionic gelation method to obtain cationic polymeric chitosan-tripolyphosphate nanoparticles. *Int J Pharm*. 2013;446(1–2):199–204.
35. Li J, Huang Q. Rheological properties of chitosan-tripolyphosphate complexes: from suspensions to microgels. *Carbohydr Polym*. 2012;87(2):1670–1677.
36. Konecsni K, Low NH, Nickerson MT. Chitosan-tripolyphosphate submicron particles as the carrier of entrapped rutin. *Food Chem*. 2012;134(4):1775–1779.
37. Hu B, Pan C, Sun Y, Hou Z, Ye H, Zeng X. Optimization of fabrication parameters to produce chitosan-tripolyphosphate nanoparticles for delivery of tea catechins. *J Agric Food Chem*. 2008;56(16):7451–7458.
38. Singh R, Lillard JW Jr. Nanoparticle-based targeted drug delivery. *Exp Mol Pathol*. 2009;86(3):215–223.
39. Reyes-Ortega F, Rodríguez G, Aguilar MR, et al. Encapsulation of low molecular weight heparin (bemiparin) into polymeric nanoparticles obtained from cationic block copolymers: properties and cell activity. *J Mater Chem B Mater Biol Med*. 2013;1:850–860.
40. Zhang H, Hussain I, Brust M, Butler MF, Rannard SP, Cooper AI. Aligned two- and three-dimensional structures by directional freezing of polymers and nanoparticles. *Nat Mater*. 2005;4(10):787–793.
41. Deville S, Saiz E, Nalla RK, Tomsia AP. Freezing as a path to build complex composites. *Science*. 2006;311(5760):515–518.
42. Aranaz I, Gutiérrez MC, Ferrer ML, del Monte F. Preparation of chitosan nanocomposites with a macroporous structure by unidirectional freezing and subsequent freeze-drying. *Mar Drugs*. 2014;12(11):5619–5642.
43. Jia S, Yang X, Song W, et al. Incorporation of osteogenic and angiogenic small interfering RNAs into chitosan sponge for bone tissue engineering. *Int J Nanomedicine*. 2014;9:5307–5316.
44. Noel SP, Courtney HS, Bumgardner JD, Haggard WO. Chitosan sponges to locally deliver amikacin and vancomycin: a pilot in vitro evaluation. *Clin Orthop Relat Res*. 2010;468(8):2074–2080.
45. Smith JK, Moshref AR, Jennings JA, Courtney HS, Haggard WO. Chitosan sponges for local synergistic infection therapy: a pilot study. *Clin Orthop Relat Res*. 2013;471(10):3158–3164.
46. Sylvester PW. Optimization of the tetrazolium dye (MTT) colorimetric assay for cellular growth and viability. In: Satyanarayanajois SD, editor. *Drug Design and Discovery. Methods and Protocols*. Los Angeles, CA: Humana Press; 2011:157–168.
47. International Organization for Standardization. *ISO10993-5. Biological Evaluation of Medical Devices – Part 5: Tests for In Vitro Cytotoxicity*. Geneva, Switzerland: International Organization for Standardization; 2009:1–34.
48. Heim KE, Tagliaferro AR, Bobilya DJ. Flavonoid antioxidants: chemistry, metabolism and structure-activity relationships. *J Nutr Biochem*. 2002;13(10):572–584.
49. Bors W, Michel C, Schikora S. Interaction of flavonoids with ascorbate and determination of their univalent redox potentials: a pulse radiolysis study. *Free Radic Biol Med*. 1995;19(1):45–52.
50. Procházková D, Boušová I, Wilhelmová N. Antioxidant and prooxidant properties of flavonoids. *Fitoterapia*. 2011;82(4):513–523.
51. Zhang Y, Yang Y, Tang K, Hu X, Zou G. Physicochemical characterization and antioxidant activity of quercetin-loaded chitosan nanoparticles. *J Appl Polym Sci*. 2008;107(2):891–897.
52. Glavin GB, Szabo S. Experimental gastric mucosal injury: laboratory models reveal mechanisms of pathogenesis and new therapeutic strategies. *FASEB J*. 1992;6(3):825–831.
53. Al Mofleh IA. Spices as alternative agents for gastric ulcer prevention and treatment. In: Chai J, editor. *Peptic Ulcer Disease*. Rijeka, Croatia: InTech; 2011:351–374.

54. Jorge MP. *Atividade cicatrizante de microencapsulados de extrato bruto etanólico obtido de Arrabidaea chica* (*HUMB. & BONPL.*) *Verlot*. [*Wound healing activity of microencapsulated of crude ethanolic extract obtained from Arrabidaea chica* (*HUMB. & BONPL.*) *Verlot*.] [master's thesis]. Campinas: Universidade Estadual de Campinas, Faculdade de Ciências Médicas; 2013. Brazil.
55. Strasser M, Noriega P, Löbenberg R, Bou-Chacra N, Bacchi EM. Anti-ulcerogenic potential activity of free and nanoencapsulated Passiflora serratodigitata L. extracts. *Biomed Res Int*. 2014;2014:434067.
56. Suleyman H, Albayrak A, Bilici M, Cadirci E, Halici Z. Different mechanisms in formation and prevention of indomethacin-induced gastric ulcers. *Inflammation*. 2010;33(4):224–234.

Supplementary materials

Fourier transform infrared spectroscopy fitted with attenuated total reflectance

Attenuated total reflectance Fourier transform infrared spectroscopy (ATR-FTIR) spectra were recorded on a PerkinElmer Spectrum One spectrophotometer (PerkinElmer Inc., Waltham, MA, USA). Infrared spectra were obtained between 4,000 cm^{-1} and 650 cm^{-1} by 32 scans and with a scanning resolution of 4 cm^{-1}.

FTIR characterization of nanoparticle systems

The FTIR spectra (Figure S1) of nanoparticle (NP) systems loaded with *Arrabidaea chia* extract (AcE) showed the characteristic bands of its main components, chitosan and AcE.

The spectrum of AcE showed typical aromatic bands, belonging to aromatic rings, at 1,580 cm^{-1}. Empty NPs formed by partially cross-linked chitosan showed the stretching hydroxyl and amino bands at 3,414 cm^{-1} and 3,215 cm^{-1}, respectively. At 2,884 cm^{-1}, it can be observed that the stretching bands of C–H bonds belong to the chain polymer. The characteristic carbonyl (C=O) and amino (N–H) tension and torsion bands appeared at 1,664 cm^{-1} and 1,574 cm^{-1}, respectively. At 1,423 cm^{-1}, it showed the torsion band of the $-CH_2-$ groups, and at 1,316 cm^{-1}, the C–N tension band appeared. The symmetric stretching belonging to the C–O group appeared at 1,074 cm^{-1} and the glycoside bond (C–O–C) showed stretching bands at 894 cm^{-1} and 705 cm^{-1}. In the AcE-loaded NP spectrum, a slight deviation of the hydroxyl (OH) and amino (NH_2) bands was observed, appearing at 3,200 cm^{-1}, which corresponds to a mean value between the empty NP (3,260 cm^{-1}) and AcE (3,198 cm^{-1}) bands. C–H stretching bands of the chain polymer appeared at higher wave numbers (2,924 cm^{-1}) due to the presence of a positive oxygen in the AcE structure. Besides, the carbonyl and amino tension and torsion bands of chitosan were nearly overlapped in the AcE-loaded NP spectrum due to the influence of aromatic ring bands belonging to AcE.

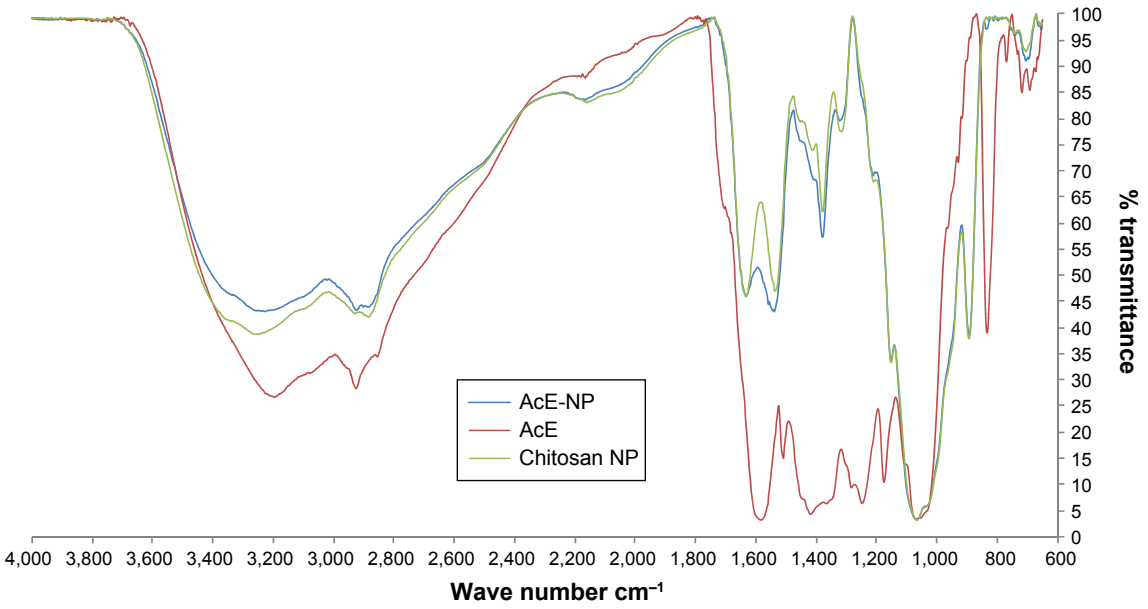

Figure S1 Fourier transform infrared spectra of AcE, chitosan NPs, and AcE-NPs.
Abbreviations: AcE-NP, *Arrabidaea chica* extract nanoparticle; AcE, *Arrabidaea chica* extract; NP, nanoparticle.

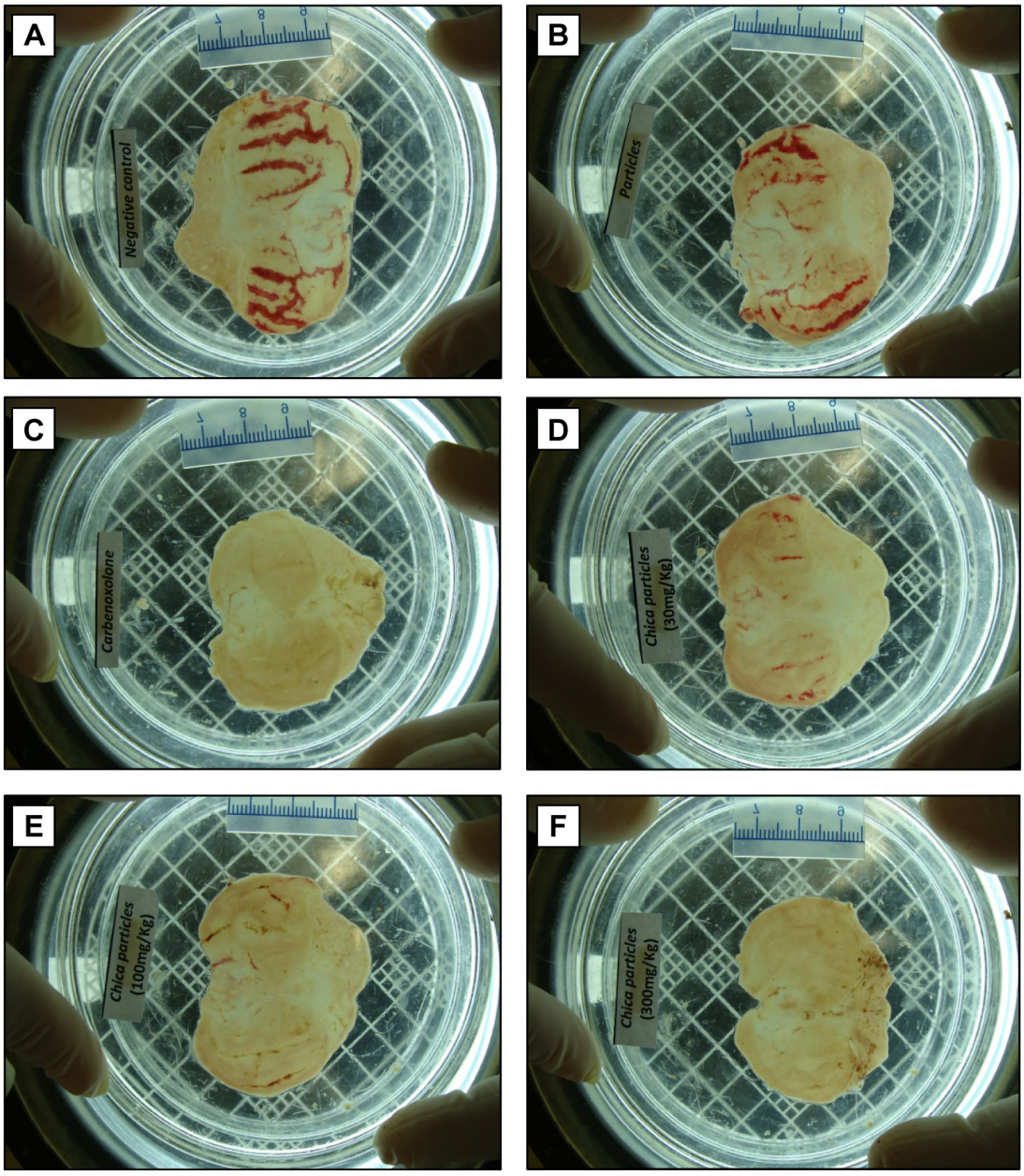

Figure S2 Stomachs opened along the greater curvature in ethanol-induced gastric ulcer.
Notes: Stomachs of rats orally pretreated with (**A**) negative control, (**B**) nonloaded nanoparticles, (**C**) carbenoxolone, and *Arrabidaea chica* nanoparticles at (**D**) 30 mg·kg^{-1}, (**E**) 100 mg·kg^{-1}, and (**F**) 300 mg·kg^{-1} doses.